DESIGN AND ATTITUDE CONTROL OF A SATELLITE WITH VARIABLE GEOMETRY

Miguel Fragoso Garrido de Matos Lino*

The rigid body dynamics equations are rewritten to obtain a general form of the Euler equations, where the shape changing capability of the body is taken into account. We envision several simple models for satellite geometries that are able to modify its shape. The inertia tensors of the geometries are determined as function of the satellite's configuration. The configuration changing capability of one of the satellite geometries is applied to achieve synchronous rotation in an elliptic orbit. The possibility of one of the envisioned satellites of changing the three moments of inertia was explored, as well as to assess the stability of rotation around the principal axes.

1. INTRODUCTION

We explore an alternative attitude control method to conventional orientation control mechanisms such as momentum wheels or thrusters - control by varying the satellite's configuration. A satellite with variable geometry would be composed by movable parts whose motion is controlled by the action of actuators. The movable parts, which could be solar panels, hardware storage containers or any other spacecraft component that could be convenient to use for this purpose, would be articulated with other components of the satellite that are fixed in the satellite's frame. The fixed parts only have rigid-body motion, unlike the movable parts that also experience motion controlled by spacecraft's actuators..

The chaotic behavior of the motion of bodies with one time-varying principal moment of inertia was addressed [3,4]. Unlike the present work, these works do not refer the spacecraft design that would allow for such a variation of the moment of inertia or consider consequences of varying one moment of inertia in other components of the inertia tensor. Other limitation is that the variation of one of the principal inertia moments is considered as a mode of representing the satellite as a deformable rigid-body and not as a method to control the satellite's attitude. Moreover, the chaos phenomena in gyrostats [3] and the chaotic modes of motion of an unbalanced gyrostat [4] have been addressed. Other related topic concerns the dynamics of gyrostats with variable inertia properties, namely the consequences in the phase space of such dynamic, without referring to the issue of chaotic behavior. The changes in angular motion due to variable mass and variable inertia of gyrostat composed by multiple coaxial bodies has already been investigated [5]. In addition, the free motion of a dual-spin satellite composed of a platform and a rotor with variable moments of inertia has been addressed [6]. The present work differs from these studies in the geometry studied, since they only consider the particular case of non-variable geometry gyrostats.

The possibility of varying mass, via jets or thrusters, has been considered [7]. However, the interpretation of additional terms that appear in the Euler equations due to the configuration variation is limited.

Other works consider two-tethered systems modelled as a variable length thin rod connecting two endpoint masses. It has been proven that a length function for a tethered system in a Moon-Earth system exists so that the rod has a constant angle with respect to the Moon-Earth direction [8]. In addition, a length function for an uniform rotation for a two-tethered body in an elliptic orbit was obtained, as well as the motion stability intervals for parameters such as eccentricity [9].

*under the supervision of P. J. S. Gil

1. ATTITUDE DYNAMICS OF A VARIABLE GEOMETRY BODY

General Euler Equations in the Principal Frame

Since there is no reference frame with respect to which a variable-geometry body mass distribution is constant during a configuration change, the body frame selected should be as convenient as possible. In this work, we selected the principal frame to be the body frame at all times. In addition, the body frame will be centered at the center of mass of the body.

We define the torque $\boldsymbol{M}$, the angular velocity $\boldsymbol{\omega}$, the inertia tensor $\boldsymbol{I}$, and the principal moments of inertia are A, B and C, with respect to x, y and z axes, respectively. A general form of the Euler equations in the three directions of the principal frame, which is centered at the center of mass, can be obtained:

$$M_x = \dot{A}\omega_x + A\dot{\omega}_x + \omega_y\omega_z(C-B) + \dot{\gamma}_x + \gamma_z\omega_y - \gamma_y\omega_z, \quad (1.1)$$

$$M_y = \dot{B}\omega_y + B\dot{\omega}_y + \omega_x\omega_z(A-C) + \dot{\gamma}_y + \gamma_x\omega_z - \gamma_z\omega_x, \quad (1.2)$$

$$M_z = \dot{C}\omega_z + C\dot{\omega}_z + \omega_x\omega_y(B-A) + \dot{\gamma}_z + \gamma_y\omega_x - \gamma_x\omega_y, \quad (1.3)$$

where we simplified the notation by defining the non-rigid term:

$$\boldsymbol{\gamma} = \int_{\Omega} \boldsymbol{r} \times {}^{B}\frac{d\boldsymbol{r}}{dt} dm, \quad (1.4)$$

being $\boldsymbol{r}$ the position with respect to the body frame of the particles of the variable-geometry body Ω, and ${}^{B}\frac{d\boldsymbol{r}}{dt}$ the time-derivative measured in the body frame.

When the geometry is constant in the body frame, we have that ${}^{B}\frac{d\boldsymbol{r}}{dt} = 0$, which implies that not only do the terms of $\dot{\boldsymbol{\gamma}}$ vanish, but the terms ${}^{B}\frac{d}{dt}(\boldsymbol{I}) \circ \boldsymbol{\omega}$ vanish as well in (1.1)-(1.3).

$\boldsymbol{\gamma}$ is related with changes in symmetries and accounts for changes in the orientation of the principal axes. In addition, $\boldsymbol{\gamma}$ can be understood as the angular momentum of the body as measured by the body frame. When the body geometry is varying, $\boldsymbol{\gamma}$ has the direction of the part of the total angular momentum that the body frame rotation does not account for.

In this work, we will consider the general form of Euler equations (1.1)-(1.3) where the variable-geometry body is not subject of any applied torques – the satellite is considered a free body in space.

Kinetic Energy and Angular Momentum

The total kinetic energy of the variable-geometry body has the rigid body component

$$T_r = \frac{1}{2} m\dot{\boldsymbol{R}}_{\boldsymbol{0}}^2 + \frac{1}{2}\boldsymbol{\omega}.(\boldsymbol{I} \circ \boldsymbol{\omega}), \quad (1.5)$$

and the non-rigid component of the kinetic energy

$$T_{nr} = \frac{1}{2}\int_{\Omega} {}^{B}\frac{d\boldsymbol{r}}{dt}.{}^{B}\frac{d\boldsymbol{r}}{dt} dm + \dot{\boldsymbol{R}}_{\boldsymbol{0}}.\int_{\Omega} {}^{B}\frac{d\boldsymbol{r}}{dt} dm + \boldsymbol{\omega}.\boldsymbol{\gamma}, \quad (1.6)$$

where $\dot{\boldsymbol{R}}_0$ is the velocity of the origin of the body frame. The first term of (1.6) is the pure non-rigid motion term. Its value is the same regardless of the rigid motion of the body, both translation and rotation: it only depends on the configuration change and hence on the distribution of the velocity with respect to the body frame ${}^{B}\frac{d\boldsymbol{r}}{dt}$, being always a non-negative term.

However, the other two other terms can be negative because they depend on the translational or rotational work the actuators are performing on the mechanical system. The term $\dot{\boldsymbol{R}}_{\boldsymbol{0}}.\int_{\Omega} {}^{B}\frac{d\boldsymbol{r}}{dt} dm$ depends on the translational state of the body and the geometry variation, expressing the translational work the actuators perform on the

body. The physical meaning of $\boldsymbol{\omega}.\boldsymbol{\gamma}$ is similar: $\boldsymbol{\omega}.\boldsymbol{\gamma}$ is positive when the actuating forces are such that the positive rotational work is being done to the system, speeding up the rotation and increasing its rotational kinetic energy.

While varying the geometry of a certain free body can changes its energy, it does not change the angular momentum. The reason for that difference is that the forces responsible for changing the geometry of the body are internal to the mechanical system considered but the energy sources responsible for that do not belong to the mechanical system – they are external. Consequently, the actuators are able to change the mechanical energy of the system but not its angular momentum.

Euler angular velocities

Defining the precession angle ψ, the nutation angle θ and the spin angle φ, it is possible to obtain separate equations for the Euler angular velocities for the free variable-geometry body, when we align the Z axis of the inertia frame with the angular momentum $\boldsymbol{h}$:

$$\dot{\theta} = h\left(\frac{1}{A(t)} - \frac{1}{B(t)}\right)\sin\theta\sin\varphi\cos\varphi, \quad (1.7)$$

$$\dot{\psi} = h\left(\frac{\sin^2\varphi}{A(t)} + \frac{\cos^2\varphi}{B(t)}\right), \quad (1.8)$$

$$\dot{\varphi} = h\cos\theta\left(\frac{1}{C(t)} - \frac{\sin^2\varphi}{A(t)} - \frac{\cos^2\varphi}{B(t)}\right), \quad (1.9)$$

where h is the norm of the angular momentum and the symmetry of the body is such that $\boldsymbol{\gamma}$ is null.

A variable geometry-body can still be axisymmetric even though its moments of inertia vary: as long as $A(t) = B(t) \neq C(t)$. Axisymmetry simplifies (1.7) to have $\dot{\theta} = 0$ implying that the variable geometry body with $\boldsymbol{\gamma} = 0$ has a constant nutation angle, regardless of how the principal moments of inertia vary with time. Consequently, the nutation angle of an axisymmetric variable-geometry can't be controlled by configuration changing, depending only on the initial conditions of the body dynamics.

2. DESIGN OF VARIABLE GEOMETRY SATELLITES

The geometries envisioned are rough approximations of possible real variable-geometry satellites so that insightful information about their dynamics may be obtained easily. For that reason, satellites are approximated by being made of very simple components: uniform slender bars, springs or point masses. We also avoided considering geometries with numerous degrees of freedom regarding the shape-changing motion which would difficult the mathematical treatment – geometries with one degree of freedom were preferred, being the degree of freedom defined as α in all geometries.

In addition, the geometries are such that have $\boldsymbol{\gamma} = 0$ at all times, which significantly simplifies the equations. This is valid because it can be proved that for a body that permanently has at least two perpendicular symmetry planes whose intersection contains the body frame's origin, which occurs for all the geometries considered in this work, has $\boldsymbol{\gamma} = 0$ and hence $\dot{\boldsymbol{\gamma}} = 0$ for all configurations.

The selected body frames for the satellites will be principal frames centered at the center of mass for all configurations.

Connected Scissor Mechanism

The Connected Scissor Mechanism was conceived as being composed by a certain even number of bars, a total of $2n$, with $n \geq 3$. The bars are slender and are articulated to each other, held together on the both ends by negligible mass joints, connected in such a way that they form a closed loop of bars.

The single degree of freedom of this geometry is the inclination of the bars: n bars have an inclination of $+\alpha$ angle and the other n bars have an inclination of $-\alpha$ with respect to the transversal symmetry plane.

The body frame used for the Connected Scissor Mechanism is oriented so that, from both the top perspective and bottom perspective of the z axis, the bar structure is seen as a regular polygon of n sides. The z axis intersects the geometrical center of the top polygon formed by the slender bars upper ends and intersects the geometrical center of the bottom polygon formed by the slender bars bottom ends.

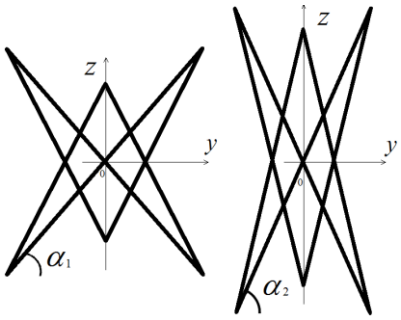

Figure 1 – Lateral perspective from the x axis of a Connected Scissor Mechanism of 6 bars.

In the $x0y$ plane, which is the transversal plane of symmetry, n orientations of the x and y axes exist so that A and B don't change between the n frames, because of the top/bottom polygon's regularity. According to the Mohr Circle [10], for the two dimensional tensor of the moments of inertia, two orientations of the x and y axes allow for a maximum A and minimum B and vice-versa, separated by an angle of amplitude of $\frac{\pi}{2}$. In this case, we have $n \geq 3$ equivalent inertia tensors in the plane. Therefore, if n orientations have the same inertia tensor then all possible frames in the $x0y$ plane have the same inertia tensor. This implies the axisymmetry $A = B$, because the maximum and minimum moments of inertia have to be equal for this to occur. Taking this into account, we obtained the moments of inertia of the geometry:

$$A = \frac{nml^2}{12}(\cos^2\alpha\,(3\tan^2\phi - 1) + 2), \quad (2.1)$$

$$C = \frac{nml^2}{6}\cos^2\alpha(1 + 3\tan^2\phi), \quad (2.2)$$

where the angle ϕ is a parameter that only depends on the number of bars

$$\phi = \pi\frac{n-2}{2n}. \quad (2.3)$$

The dependence of α in A vanishes when $\tan^2\phi = \frac{1}{3}$, which can be solved to conclude that it is only possible for $n = 3$, corresponding to the situation where the polygon is a triangle. If a number of bars larger than 6 is selected, A also varies with the degree of freedom α allowing for more options in what concerns attitude control.

Dandelion

This geometry consists in a central bar of mass M and length L and by n other bars of mass m and length l that have their top end articulated to the top end of the central bar. The n bars are equivalently spaced and form the same angle α with the central bar. The attitude control is made by changing α, the single degree of freedom of this geometry. α is limited between 0 and π.

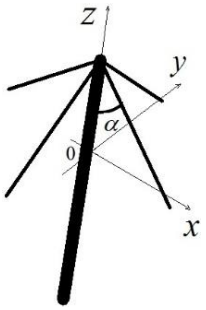

Figure 2 – Dandelion with $n = 4$ bars.

We select a body frame where the z axis is aligned with the central bar and is centered at the center of mass of the geometry.

The distance between the center of mass and the top point of the central bar is

$$z_{CM}(\alpha) = \frac{ML + nml\cos\alpha}{2(M + nm)}. \quad (2.4)$$

The origin of the body frame has the motion along the z axis prescribed by (2.4).

Taking into account the motion of the center of mass, we obtained the moments of inertia:

$$A = B = \frac{nml\cos\alpha\,(l\cos\alpha\,(4M + nm) - 6ML)}{12(M + mn)} + \frac{ML^2(M + 4nm)}{12(M + mn)} \quad (2.5)$$

$$C = \frac{nml^2}{3}\sin^2\alpha. \quad (2.6)$$

Eight Point Masses

This concept consists in having the attitude control of the satellite be performed by prescribing the variation of C, while keeping the other two constant.

The variation of C is achieved by the controlled motion eight masses m along a specified trajectory within its respective tube. The tubes are regarded as having negligible mass comparing with the masses. The eight masses and the structure required for it are an installation in the satellite to control its attitude rather than a model for a satellite itself.

The eight-mass system as a whole is conceived as having a single degree of freedom because the position of the masses are given by the mirrored positions of the other masses, for all configurations.

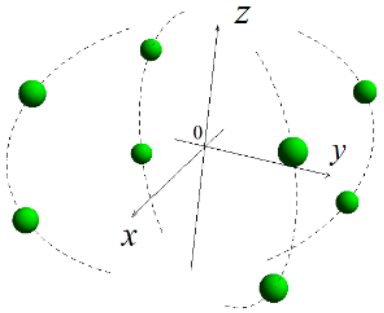

Figure 3 – Eight Point Masses in space.

The selected body frame for this geometry has the coordinate planes $x0y, y0z$ and $x0z$ be the symmetry planes of the masses motion. The eight masses can be regarded as vertexes of a parallelepiped that can change its shape. Each of the faces of the parallelepiped is intersected at the respective geometric center by a coordinate axis, as can be observed in Figure 3.

We define that the coordinates of the point mass that belongs to the first octant are x, y, z, being the positions of the other seven masses given by mirrored position of this one.

So that the body is axisymmetric, we define the single degree of freedom as being given

$$\alpha(t) = x(t) = y(t), \quad (2.7)$$

for any instant t, while the third coordinate is $z(t)$. The moments of inertia are:

$$A = B = 8m(\alpha^2 + z^2), \quad (2.8)$$

$$C = 16m\alpha^2. \quad (2.9)$$

It can be concluded that the allowed trajectories for the eight masses belong to the planes $x = y$ and $x = -y$ form an ellipse in three-dimensional space, one for each of plane. The ellipse is tapered in the horizontal direction, along $x = y$ or $x = -y$.

A downside of having variable-geometry axisymmetric satellites as the Connected Scissor Mechanism, the Dandelion and the Eight Point Masses with $A = B$, is that the nutation angle is not controllable. In addition, for the Connected Scissor Mechanism geometries, which was the single geometry where it was possible to obtain $\frac{dA}{d\alpha} = 0$ for all α when $n = 3$, the precession rate $\dot{\psi}$ is not controllable as well.

Compass

The compass has variable moments of inertia such that $A \neq B \neq C$ in order to allow for a less limited attitude control than the already discussed geometries.

The Compass consists of two bars articulated at one joint, where one end of each bar coincides. Its degree of freedom is the opening angle around the joint, 2α. In this work, we limited the range of α to $0 \leq \alpha \leq \pi$, but it would be interesting to explore the possibilities of having an unlimited range of α. The bars are

uniform and slender, having mass m and length l.

The $y0z$ plane contains both the bars and z axis is a symmetry axis, having its positive direction pointing towards the joint.

The position of the center of mass with respect to the joint depends on the aperture α, which is taken into account to determine the moments of inertia, since the body frame is centered at the moving center of mass.

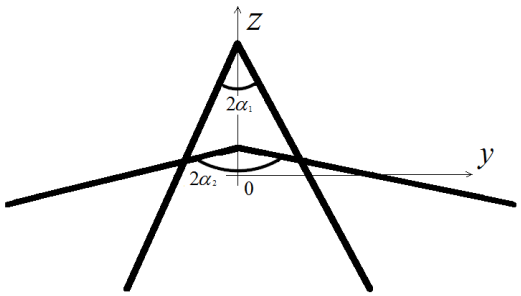

Figure 4 – Compass for two different configurations, α_2 and α_1, with $\alpha_2 > \alpha_1$.

The moments of inertia are:

$$A = \frac{ml^2}{6}(3\sin^2\alpha + 1), \qquad (2.10)$$

$$B = \frac{ml^2}{6}\cos^2\alpha, \qquad (2.11)$$

$$C = 4\frac{ml^2}{6}\sin^2\alpha. \qquad (2.12)$$

3. SOLUTIONS OF THE FREE VARIABLE-GEOMETRY SATELLITE MOTION

Synchronous Rotation in an Elliptical Orbit with a Variable-Geometry Satellite

An interesting application of the variable-geometry satellites presented in this work could be to use the configuration change to have a synchronous rotation throughout an elliptic orbit. Since the velocity of a satellite is not constant during the orbital period in an elliptic orbit, the configuration of the geometry as function of time would be such that the precession rate is synchronized with the movement of the satellite in the orbital plane. We consider small eccentricity orbits, $e \leq 0.1$, that require small geometry variations from the satellite.

The Connected Scissor Mechanism was selected to explore this application because this geometry, being axisymmetric, can change its moment of inertia A and therefore is able to control the precession rate as intended. In addition, it is versatile and has simpler expressions for the moment of inertia A (2.1) when compared to the equivalent expression for the Dandelion (2.5).

The condition for having the rotation of the satellite be synchronous with the movement in the orbital plane is satisfied by having

$$\dot{f} = \dot{\psi} \qquad (3.1)$$

during all instants of an orbital period, being f the true anomaly. The mean angular velocity of the orbit is ν.

Using an analytical approximation for $\dot{f}(t)$, where terms on e^2 where neglected, we obtained the configuration of the satellite as function of time $\alpha(t)$ that satisfies (3.1):

$$\alpha(t) = \arccos\sqrt{\frac{k\cos^2\alpha_0 + 2}{k}g - \frac{2}{k}}, \qquad (3.2)$$

where $g(t)$ is given by

$$g(t) = \left(\frac{e\cos(\nu t + e\sin(\nu t)) - 1}{e - 1}\right)^2, \qquad (3.3)$$

and

$$k = 3\tan^2\left(\pi\frac{n-2}{2n}\right) - 1, \qquad (3.4)$$

which is a constant value that depends only on the number of bars selected.

We arbitrated that the initial conditions in (3.2) correspond to the passing of the satellite by the periapsis at $f = 0$ with a configuration α_0,

being this the first instant when the $\dot{\psi} = \dot{f}$ begins to be satisfied. Nevertheless, we could select any other point in the orbit to use its conditions as reference.

Expression (3.2) may not be possible for certain combinations of parameters. The condition so that the synchronous rotation is possible solution throughout the orbital period is

$$\cos^2 \alpha_0 \leq \frac{(1-e)^2 - \frac{8e}{k}}{(1+e)^2}, \qquad (3.5)$$

where we observe the angle α_0 can be allowed to have any value larger than a certain minimum α_0 that depends on e and k.

It is possible to assess how the minimum α_0 varies with e and k by plotting different curves of α_0 as function of e for different number of bars.

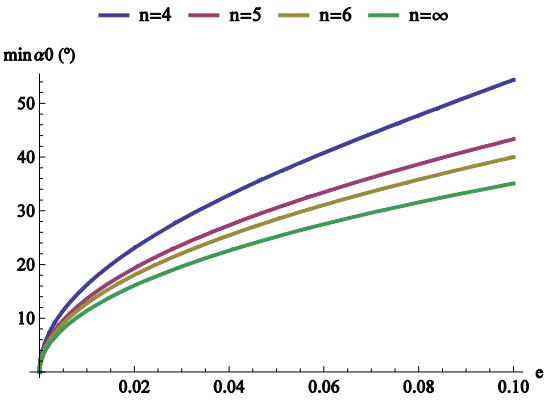

Figure 5 - Minimum α_0 as function of the eccentricity of the orbit for different number of bars.

We observe from Figure 5 that the range of possible α_0 becomes more limited with the increase in eccentricity. On the other hand, increasing the number of bars decreases the minimum α_0 allowed, since the curves in Figure 5 get lower with larger n, until the theoretical limit of $n = \infty$. Consequently, the most limiting situation is having the minimum number of bars, $n = 4$ and having the highest eccentricity $e = 0.1$, which corresponds to a minimum α_0 of $54.4°$, which still leaves almost half of the total range of α available.

We obtain $\alpha(t)$ graphically for the particular example of a geosynchronous orbit, with $\nu = 7.292 \times 10^{-5}\ \mathrm{rad/s}$ [11].

In order to observe the influence of the parameters α_0, n and e in the configuration as function of time $\alpha(t)$, we selected two different values for each of the parameters.

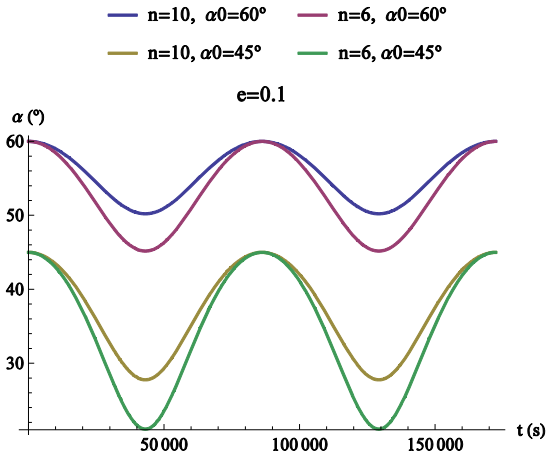

Figure 6 – $\alpha(t)$ with $e = 0.1$ during two sidereal days.

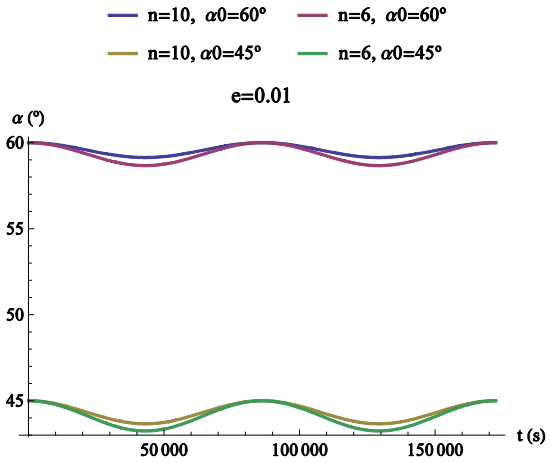

Figure 7 – $\alpha(t)$ with $e = 0.01$ during two sidereal days.

We observe in Figure 6 and in Figure 7 that $\alpha(t)$ is a periodic function with a period equal to the orbital period, which is in this case a sidereal day.

$\alpha(t)$ has the maximum value at the periapsis, where the orbital velocity is maximum, and the minimum value at the apoapsis, where the orbital velocity is minimum. For the synchronous rotation to occur, the maximum and minimum of the orbital speed of the precession rate must coincide and, consequently, the precession rate must be maximum at the periapsis and minimum at the apoapsis, which implies minimum A at the periapsis and maximum A at the apoapsis, according to (1.8) for the axisymmetric case. Since A of the Closed Scissor Mechanism increases when α decreases (2.1), the minimum α has the maximum at the periapsis and the maximum at the apoapsis, which is confirmed by Figure 6 and Figure 7.

Higher eccentricities imply larger configuration changes during an orbital period, because larger orbital velocity variations occur during a period, implying therefore larger changes in the inertia tensor. Increasing the number of bars results into having a smaller required amplitude of configuration change.

Moments of Inertia Swap

The geometry that offers the widest range of control possibilities by configuration changing is the Compass, because the three moments of inertia are variable.

Even though A is the largest of the principal moments of inertia for all configurations, the intermediate and the smallest of the moments of inertia depend on α. We have that $B > C$, for $0 < \alpha < \alpha_C \cup \pi - \alpha_c < \alpha < \pi$ and $B < C$ for $\alpha_C < \alpha < \pi - \alpha_C$, being the critical angle given by $\alpha_C = \arcsin(1/\sqrt{5})$.

We determine the derivatives of the principal moments of inertia by differentiating (2.10)-(2.12) and insert the derivatives and the moments of inertia (2.10)-(2.12) into (1.1)-(1.3), for a free-body with $\boldsymbol{\gamma} = 0$.

The resultant system of differential equations is non-linear and coupled.

We could only find an approximated solution around $\alpha = \alpha_C$, for $\omega_z \sim 1\,\mathrm{rad/s}$ being $\omega_z \gg \omega_y, \omega_z$, with $\omega_y, \omega_z \sim 0.1\,\mathrm{rad/s}$:

$$\omega_x(\alpha) = \omega_x(\alpha_0)\frac{1 + 3\sin^2\alpha_0}{1 + 3\sin^2\alpha}, \qquad (3.6)$$

$$\omega_y(\alpha) = \omega_y(\alpha_0)\frac{\cos^2(\alpha_0)}{\cos^2(\alpha)}, \qquad (3.7)$$

$$\omega_z(\alpha) = \omega_z(\alpha_0)\frac{\sin^2\alpha_0}{\sin^2\alpha}, \qquad (3.8)$$

where α_0 refers to an initial condition close to $\alpha = \alpha_C$. From (3.6)-(3.8), we conclude that there is no exchange between the three components of the angular momentum, since each of the components is conserved separately.

The approximated solution also allowed to the determine the kinetic energy $T(\alpha)$, which was used to obtain the semi-axes of the ellipsoid of the kinetic energy depending on the configuration, as well as the angular momentum ellipsoid.

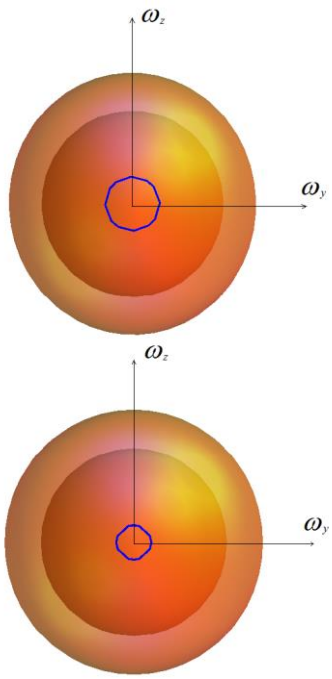

Figure 8 – Ellipsoids of angular momentum and kinetic energy for different configurations, α_0 at the top and α at the bottom.

Figure 8 shows an example of the ellipsoids for the configuration angles $\alpha_0 = 0.45$ and $\alpha = 0.47$, which are close to the critical angle $\alpha_C = 0.46$. The initial components of the angular velocity also respect the assumptions made on this section: $\omega_x(\alpha_0) = \omega_y(\alpha_0) = 0.1\ \mathrm{rad/s}$ and $\omega_z(\alpha_0) = 1\ \mathrm{rad/s}$.

Figure 8 shows nearly circular shapes, because the semi-axes of the ellipsoids on the ω_y and on the ω_z directions are very close, since α and α_0 are close to the critical configuration α_C, for which the Compass has $B = C$.

Since the relation between the moments of inertia depends on the configuration, we obtained the stable and unstable configurations of the motion of the around the three principal axes, when there is no change in configuration, which is resumed on Table 1. We verified that the axis around which the Compass can rotate stably are the axes that correspond to either the maximum moment of inertia or to the minimum moment of inertia for the current configuration, as it happens for a rigid body [7].

$\boldsymbol{\alpha} \in$	$\boldsymbol{x}$	$\boldsymbol{y}$	$\boldsymbol{z}$
$]0, \alpha_C[$	stable	unstable	stable
$]\alpha_C, \pi - \alpha_C[$	stable	stable	unstable
$]\pi - \alpha_C, \pi[$	stable	unstable	stable

Table 1 - Configurations of stability for the Compass when $\dot{\alpha} = 0$.

We also attempted to study the stability when the satellite is changing its configuration, but we concluded that assessing the stability of the rotation of the Compass around each of the principal axes is difficult, given that the terms in the dynamics matrixes are not only variable but contain non-linear functions of the configuration as well.

4. CONCLUSIONS

We concluded that the added complexity of the configuration changing is in general large, even though we could obtain some simplifying assumptions to obtain either approximations or to make the terms related with configuration changing vanish.

A wide variety of simple geometries that eliminate the extra-terms related to variable geometry to simplify the problem, but still change their inertia tensors in different ways.

It was concluded that it is possible to obtain an axisymmetric geometry made of connected slender bars where only one moment of inertia varies, even though we realized that such an inertia tensor does not allow for either precession rate or nutation rate controls.

We concluded that attaining synchronous rotation in an elliptic orbit by configuration changing is possible in most situations, being not achievable only in unrestrictive conditions. Interesting physical insight on how the configuration function depends with various parameters has been discussed by comparing graphics in different situations.

In the case of the satellite with three variable principal moments of inertia, it was observed that an interesting feature of the satellites with such a capability is to be able to swap the order of the values of the moments of inertia, being therefore possible to alter the rotation around principal axes from stable to unstable or unstable to stable. Having this feature in mind, we obtained the equations of the dynamics of this satellite, for which we could find an approximate solution around the configuration where the smaller and intermediate moments of inertia of the satellite swap.

Future work

We used simple models for the envisioned satellites as a first approach. However, for a precise description of the attitude dynamics, more detailed spacecraft models would be required.

It would be interesting to assess which components of the satellite sub-systems could be used more efficiently to perform the

secondary objective of controlling the attitude. Also, a feasibility study could be conducted in order to determine how the variable geometry attitude control method compares with conventional control methods, in terms of precision and energy expense, depending on how large the required attitude maneuvers are.

In this work, the suggested geometries had symmetries so that a variable-geometry term vanishes, in order to simplify the problem. A different approach to this would be to study the dynamics of bodies that wouldn't have such symmetries and evaluate the consequences on the attitude solutions.

Swapping the order of the values of the principal moments of inertia, as a consequence of configuration changing, can be studied in the future as a method to induce controlled instability in the rotation of an axis, which could result in an intended attitude maneuver to achieve large angle changes on the orientation of spacecraft.

5. REFERENCES

[1] M. Inarrea and V. Lanchares, "Chaotic rotations of an asymmetric body with time-dependent moments of inertia and viscous drag," *International Journal of Bifurcation and Chaos*, 2003.

[2] M. Iñarrea and V. Lanchares, "Chaotic pitch motion of an asymmetric non-rigid spacecraft with viscous drag in circular orbit," *International Journal of Non-Linear Mechanics*, vol. 41, no. 1, pp. 86–100, Jan. 2006.

[3] V. Aslanov and V. Yudintsev, "Dynamics and chaos control of gyrostat satellite," *Chaos, Solitons & Fractals*, vol. 45, no. 9–10, pp. 1100–1107, Sep. 2012.

[4] V. S. Aslanov and A. V. Doroshin, "Chaotic dynamics of an unbalanced gyrostat," *Journal of Applied Mathematics and Mechanics*, vol. 74, no. 5, pp. 524–535, Jan. 2010.

[5] A. V. Doroshin, "Analysis of attitude motion evolutions of variable mass gyrostats and coaxial rigid bodies system," *International Journal of Non-Linear Mechanics*, vol. 45, no. 2, pp. 193–205, Mar. 2010.

[6] V. S. Aslanov and V. V. Yudintsev, "Dynamics and control of dual-spin gyrostat spacecraft with changing structure," *Celestial Mechanics and Dynamical Astronomy*, vol. 115, no. 1, pp. 91–105, Nov. 2012.

[7] W. Thomson, *Introduction to Space Dynamics*, First. New York: Dover Publications, 1961.

[8] A. A. Burov, A. D. Guerman, and I. I. Kosenko, "Equilibrium Configurations and Control of a Moon-anchored Tethered System," pp. 251–266, 2013.

[9] A. A. Burov, I. I. Kosenko, and A. D. Guerman, "Uniform Rotations of a Two-body Tethered System in an Elliptic Orbit," in *64th International Astronautical Congress, Beijing, China*, 2013, pp. 1–13.

[10] F. Beer and E. R. Johnston, *Vector Mechanics for Engineers: Statics*, 6th ed. 2006.

[11] W. Wiesel, *Spaceflight Dynamics*, Second. Irwin/McGraw-Hill, 1997.